

## Modeling and Simulation of Turning Operation

M.Kumara Swamy<sup>1</sup>B.Padma Raju<sup>2</sup>B.Ravi Teja<sup>3</sup>

<sup>1</sup>Associate professor, Department of Mechanical Engineering, University College of engineering,  
JNTUK- Kakinada, A.P, INDIA

<sup>2,3</sup>PG students, Department of Mechanical Engineering, University College of engineering,  
JNTUK- Kakinada, A.P, INDIA

**Abstract:** Turning is one of the metal cutting operation, is most widely used manufacturing technique in the industry and there are lots of studies to investigate this complex process in both academic and industrial world. Metal cutting operations still represent the largest class of manufacturing operations where turning is the most commonly employed material removal process. Advances in CNC/NC machining and high speed machining technologies have boosted the productivity of machining process. One of the state of the art efforts in manufacturing engineering is to use the FEM for simulation of the metal cutting process. Simulation can increase the understanding of the cutting process and reduce the number of experiments. Researchers find these variables by using experimental techniques which makes the investigation very time consuming and expensive. At this point, finite element modeling and simulation becomes main tool. These important cutting variables can be predicted without doing any experiment with finite element method. In this study the metal cutting process is analyzed with FEM model for 3D simulation of turning process with solid single point cutting tool. This tool is modeled with CATIAV5, and exported STL files and imported in DEFORM 3D. [1]

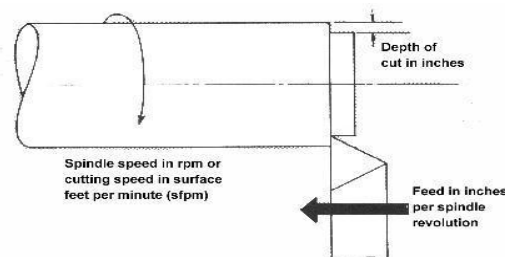
**Keywords:** CATIA, Chip formation, Deform-3D, PCBN cutting tool, turning.

### I. Introduction:

Turning is the machining operation that produces cylindrical parts. In its basic form, it can be defined as the machining of an external surface as with the workpiece rotating, with a single-point cutting tool, and with the cutting tool feeding parallel to the axis of the workpiece and at a distance that will remove the outer surface of the work. Taper turning is practically the same, except that the cutter path is at an angle to the work axis. Similarly, in contour turning, the distance of the cutter from the work axis is varied to produce the desired shape. In such setups, each tool operates independently as a single-point cutter. The three primary factors in any basic turning operation are speed, feed, and depth of cut. Other factors such as kind of material and type of tool have a large influence, of course, but these three are the ones the operator can change by adjusting the controls, right at the machine tool. Gabriela Patrascu [2] presented a FEM model for 3D simulation of turning process with chip breaker tools. The model uses Oxley's machining theory to predict cutting forces for square inserts. Inserts were modeled with CATIA V5R8 and exported as STL files into DEFORM 3D™ software. A comparison is made between predicted and experimental results showed good agreement. All worked on the FEA of machining AISI1045 steel with carbide tool. Experiments were performed at different cutting speeds i.e. 100,150,175 m/min to predict the cutting forces. The experiment results are compared with FEM results. Good correlations obtain between experiment and FEM results of shear strain.

### II. Adjustable Cutting Forces In Turning:

The three primary factors in any basic turning operation are speed, feed, and depth of cut. Other factors such as kind of material and type of tool have a large influence, of course, but these three are the ones the operator can change by adjusting the controls, right at the machine tool. All the imp parameters are shown in fig 1



Turning and the adjustable parameters  
Figure1. Parameters of turning operation

### III. Design And Modelling Of Single Point Cutting Tool:

The basic element of modern machining process consists of a machine tool, a control system, and the cutting tool. Each element may be compared to the leg of the tripod, if one leg is missing, the other two will fall. Thus a machine tool and control system are useless without cutting tool and vice versa. The primary duty of tool designer may be to select or design tools for a metal cutting operation. To select proper tool efficiently, one must have a good knowledge of the metal cutting process, be familiar with tool geometry, and be aware of types of standard tools available. It should be emphasized that standard cutting tools should be used whenever possible for reasons of economy. Single point tools are those having only one cutting edge; such as cutting tools used on lathe, shaper, planer, boring machine tools.

#### 3.1 Tool Geometry:

For cutting tools, geometry depends mainly on the properties of the tool material and the work material. The standard terminology is shown in figure 2. For single point tools, the most important angles are the rake angles and the end and side relief angles. The back rake angle affects the ability of the tool to shear the work material and form the chip. For high-speed steels, back rake angle is normally chosen in the positive range. [3-4]

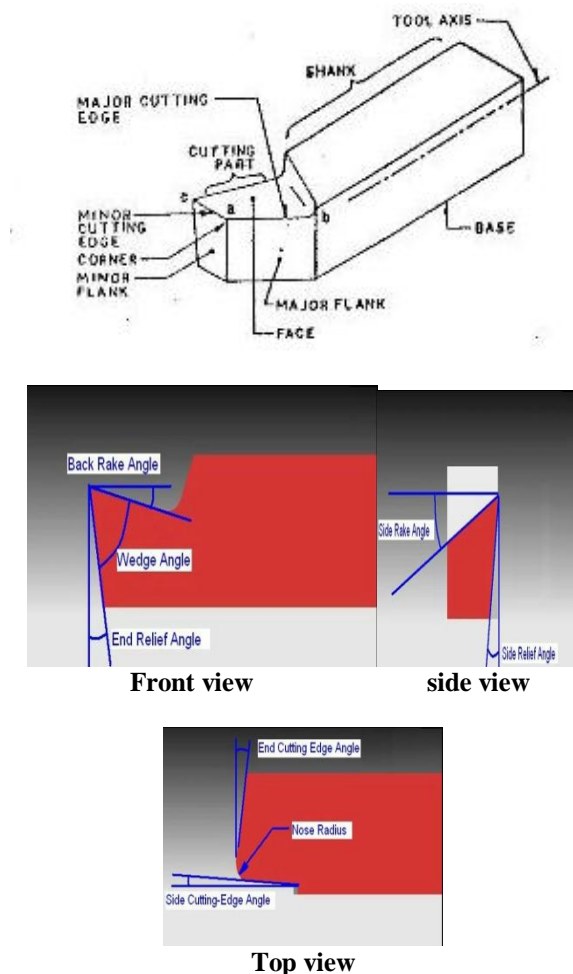


Figure2: Tool Geometry

#### 3.2 PRINCIPLE ANGLES & CUTTING FORCES OF SINGLE POINT TOOLS:

The different angles provided on single point tools play a significant role in successful and efficient machining of metals. Therefore the main angles provided on these tools are shown in Fig 2 and the average values of these cutting different metals are given as: Rake angle, Lip angle Clearance angle, Relief angle, Cutting angle.

**Calculation of Cutting Forces:**

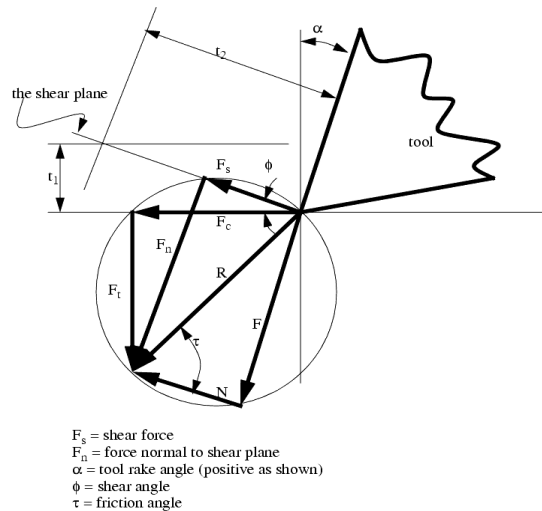


Figure3. Merchant's circle

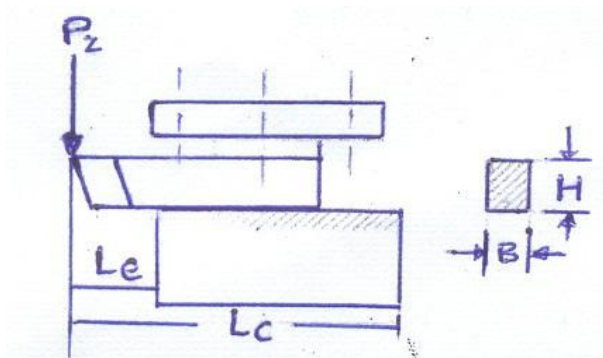


Figure4. Cutting Tool cross section

From Merchant's Circle Diagram for turning operation, we have:

**Tangential or Cutting Force:**

$b = d / \sin \lambda$ , Where,  $t_2$  = chip thickness and  $\lambda$  = principal cutting edge angle

$t = f * \sin \lambda$

$\xi$  = chip reduction coefficient =  $t_2 / t_1 = t_2 / f \sin \lambda$ , It is difficult to measure chip thickness and evaluate the values of  $\xi$  while machining brittle materials and the value of  $\tau_s$  is roughly estimated from  $\tau_s = 0.175 \text{ BHN}$

Where, BHN= Brinnel Hardness Number But most of the engineering materials are ductile in nature and even some semi brittle materials behave ductile under the cutting condition. And the value of  $\tau_s$  is obtained from,

$\tau_s = 0.186 \text{ BHN}$  ( approximate) Or,  $\tau_s = 0.74 \sigma_u \epsilon^{0.6 \Delta}$

( more suitable and accurate) [Where,  $\sigma_u$  = ultimate tensile strength of the work material  $\epsilon$  = cutting strain  $\xi - \tan \Delta = \% \text{ elongation}$

$F_c = b t \tau_s (\xi - \tan \lambda + 1)$  Longitudinal or Feed Force,  $P_x$  and Radial Force,  $P_y$

$F_z = b t \tau_s (\xi - \tan \lambda - 1) \sin \lambda$

$F_t = b t \tau_s (\xi - \tan \lambda - 1) \cos \lambda$

**IV. Design Of PCBN Cutting Tool To Machine Medium Carbon Steel Work Piece On A Lathe Machines:**

Various parameters required for modeling of a PCBN tool are listed below: [11]

BHN of work piece material = 210 Kg/ mm<sup>2</sup>

Back Rake Angle, Side Rake Angle and Side Cutting Edge Angle for PCBN tool for machining medium carbon steel are 8°, 12°, 45° respectively.

Dynamic Shear Stress of medium carbon steel can be calculated using  $\tau_s = 0.186 \text{ BHN Kg/ mm}^2$

Ultimate Tensile Strength of PCBN is  $\tau_u = 1000 \text{ N / mm}^2$  Factor of Safety for rough machining is 10.

Shank of Tool Section is Rectangle  $H=1.25B$   
 Tool over Hung Length ( $L_e$ ) is 30 mm  
 Chip Reduction Co-efficient ( $\xi$ ) is 2.5 for rough machining.  
 Depth of cut ( $d$ ) = 0.5mm  
 Feed = 0.05 mm/rev.

**4.1 MODELLING OF SINGLE POINT CUTTING TOOL USING CATIA:**

CATIA (Computer aided three dimensional interactive application) is a solid modeling tool, it unites the 3D parametric features with 2D tools, but also addresses every design through manufacturing process. The model of a single point cutting tool is quite simple.[5-6] The cutting tool model generated under part design workbench, three tools are used for this model i.e. sketcher, pad and pocket. In sketcher the actual 2D model with required dimensions is generated. The 2D model generated using sketcher is then converted into a 3D model using pad tool. Based on the tool

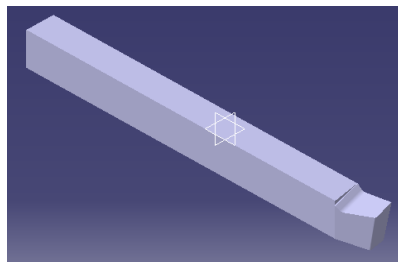


Figure5. Model of Solid single point cutting tool

Geometry views pocket tool is used to eliminate the unwanted sections.

**V. Material Properties:**

The accuracy of finite element predictions of turning operation depends greatly on the correctness of the values of material properties. A careful look into material properties of the cutting tool and the work piece are presented. Here PCBN is chosen as cutting tool material AISI 1045 steel as work piece material. Polycrystalline Cubic Boron Nitride (PCBN) cutting tools perform well during machining of hardened steels because of their high hot hardness, low solubility in iron, and good fracture toughness. They offer the possibility of greater process flexibility, reduced machining time, lower energy consumption, recycling possibilities, and the optional use of a coolant.

According to the American Iron and Steel Institute (AISI) products manuals, AISI 1045[11] Steel belongs to the alloy steel class. Steels are characterized as alloy steels when the maximum of the range specified for the content of alloying elements exceeds one or more of the following limits: Mn >0.75%, Si > 0.25%, C > 0.45%, Ph>0.050%,S>0.05%. AISI 1045 steel also falls into the Medium-carbon steel category, which is characterized by a carbon content of 1.0% or higher. It finds applications in several rotating parts like anti-friction bearings, cams, crank shaft, etc. The chemical composition of this hardened steel is listed in Table 1

Table1. Material Property for High PCBNT

Young’s modulus (GPa)	680
Poisson’s ratio	0.22
Thermal conductivity (W/m.°K)	100
Thermal Expansion co-efficient	4.9
Heat capacity	2.76
Specific heat	-
Emissivity	0.45

Table2. Material properties of AISI 1045 Steel

Temperature	20	200	400	600	800
Yield strength[MPa]	400	340	300	160	42
Ultimate Strength [MPa]	650	660	560	255	93
Young’s modulus[GPa]	215	210	165	160	90
Poisson’s ratio	0.3	0.3	0.3	0.3	0.3
Density[Kg/mm]	7930	7880	7820	7750	7720
Thermal Expansion	10.1	12.0	14.0	16.6	18

**VI. Results And Discussion:**

This study is concerned with finite element analysis of turning operation with PCBN Tool. AISI 1045 grade steel is machined with PCBN Cutting Tool.3D [7] turning operation is simulated and analyzed using FEM code DEFORM 3D.the distribution of effective stress, effective strain and strain rate in the work piece is

studied. Finite element simulations were carried out for different cutting speeds and constant depth of cut feed rates with DEFORM-3D and Theoretical calculations separately. Table 6.2 shows the different cutting speeds under which simulations [8] were carried out. From the simulations, variables like stresses, strains and temperature distribution can be obtained. However, these are all very difficult to measure experimentally.

**6.1 STUDY OF FEM SIMULATION:**

The longer the chip generation caused higher mesh displacement as shown at the end of chip formed. The biggest deformation was occurred on the primary deformation zone, followed by the secondary deformation zone [9-10]. This cause higher stress occurred in this section. This result is agreeable with findings where the major deformation during cutting process was concentrated in two regions, near to the cutting tool edge, and the biggest deformation was occurred in the primary deformation zone, followed by secondary deformation zone.

**6.2 EFFECTIVE STRESS DISTRIBUTION AT DIFFERENT CUTTING SPEEDS:**

When turning operation is carried out with AISI 1045 steel as work piece material and PCBN as cutting tool [11-13] the effective stress values are noted for different cutting feed increasing from 100 to 200 m/min. The simulated values of effective stresses are shown in figures (6.1 to 6.5) respectively. In this FEM simulation cutting tool is run on work piece up to 3.5 mm with Depth of cut – 0.5 and Feed -0.05 on all cutting speeds. While observing the captured images the higher effective stress occurred around the primary deformation zone.

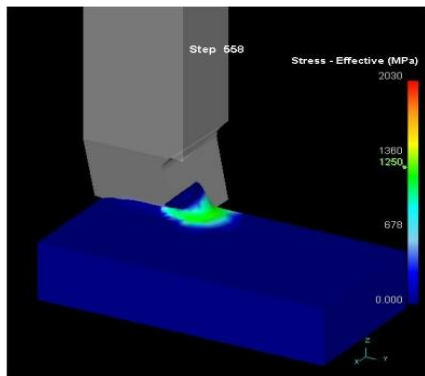


Fig 6.1: Effective stress at 100m/min

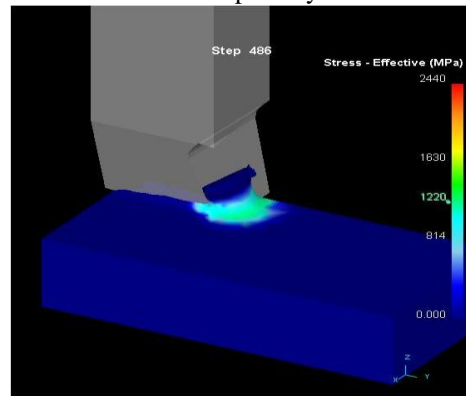


Fig 6.3: Effective stress at 150m/min

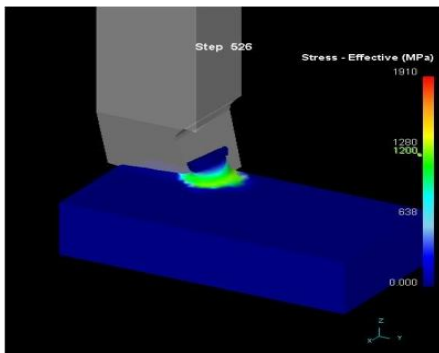


Fig 6.2: Effective stress at 125m/min

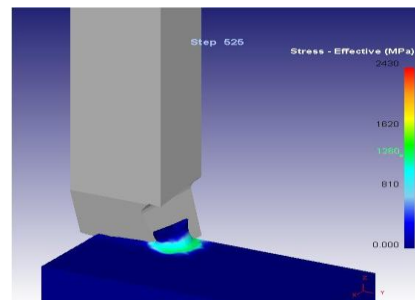


Fig 6.4: Effective stress at 175m/min

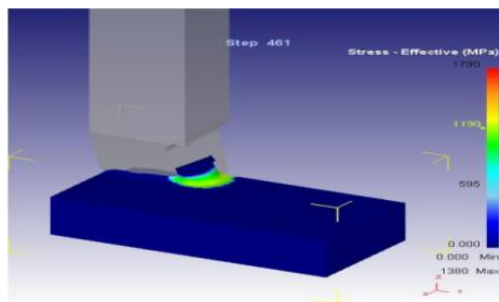


Fig 6.5: Effective stress at 200m/min

6.3 STRAIN DISTRIBUTION AT DIFFERENT CUTTING SPEEDS:

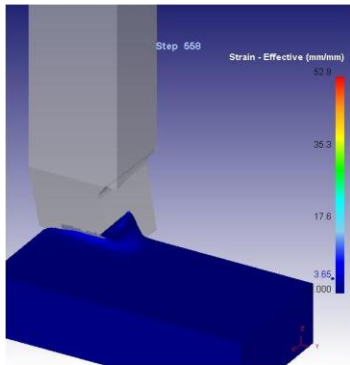


Fig 6.6: Effective strain at 100m/min

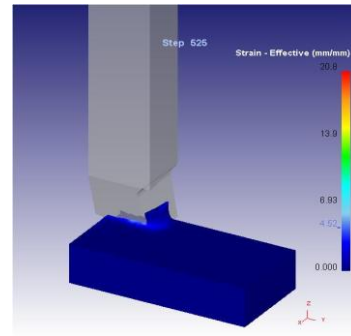


Fig 6.9: Effective strain at 175m/min

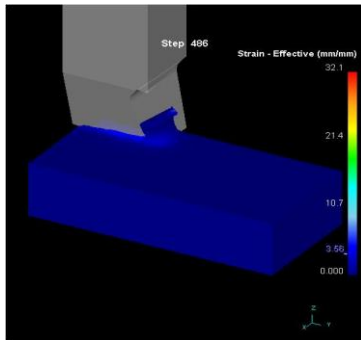


Fig 6.7: Effective strain at 125m/min

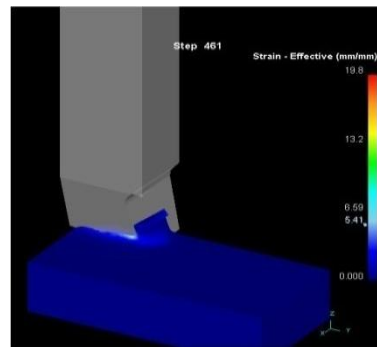


Fig 6.10: Effective strain at 200m/min

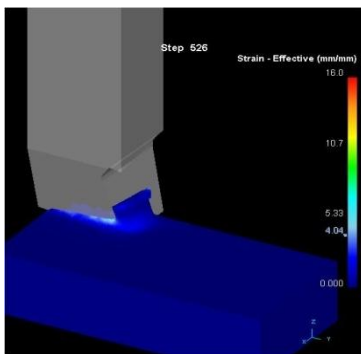


Fig 6.8: Effective strain at 150m/min

It can be seen that the effective strain is found to be maximum at the secondary shear zone. Here a region of large plastic strain exists. The secondary shear zone is also visible around the rake face in this distribution. The Maximum effective strain occurs on the rake face just above the cutting edge and the residual strain at the subsurface of the machined work piece, these decreases along the surface.

6.4 TEMPERATURE VARIATION AT DIFFERENT CUTTING SPEEDS:

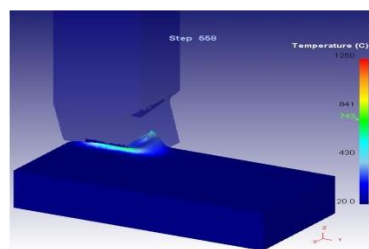


Fig 6.11: Temperature at 100m/min

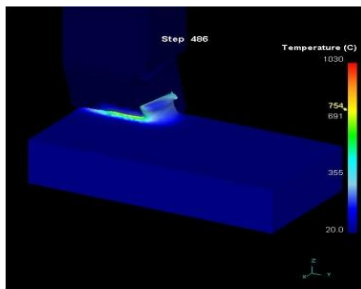


Fig 6.12: Temperature stress at 125m/min

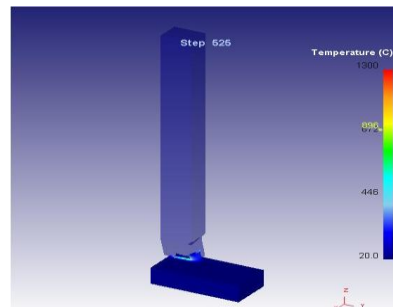


Fig 6.14: Temperature at 175m/min

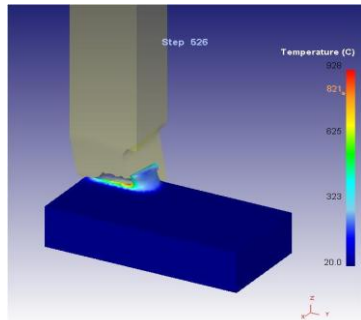


Fig 6.13: Temperature at 150m/min

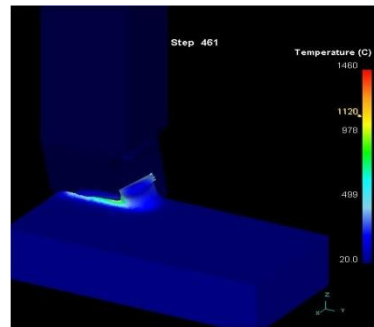


Fig 6.15: Temperature at 200m/min

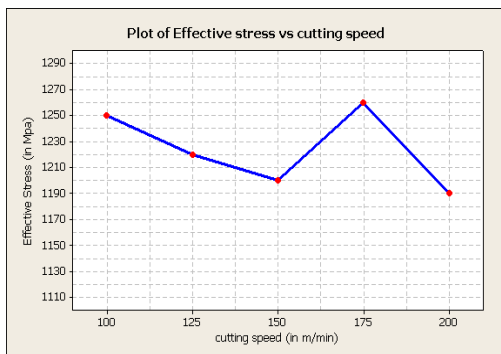
**6.5 Effect of Increasing of Cutting Speed on the effective-stress effective strain and temperature:**

The effective-stress, effective strain and chip temperature at various cutting feeds are studied and analyzed which are shown in Table 3:

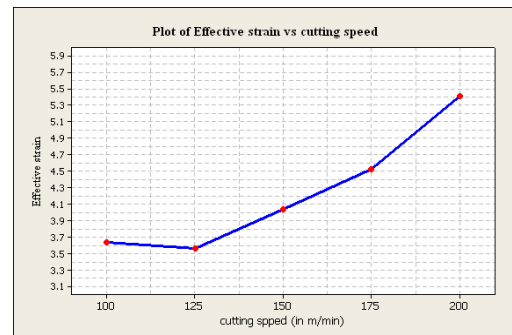
Table 3: Results for effective stress, effective strain and temperature by varying the cutting speed Whereas, Fig. 6.16, Fig 6.17 and Fig 6.18 shows simulation results at constant feed rate of 0.05 mm/rev and depth of cut of 0.5 mm.

Table 3: Results for effective stress, effective strain and temperature

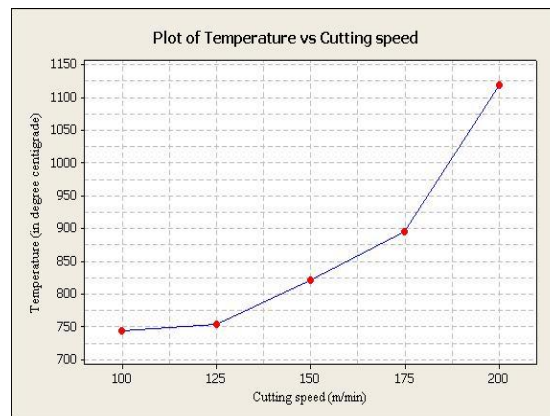
No	Cutting Speed (m/min)	Effective stress (M pa)	Effective strain	Temperature variation
1	100	1250	3.65	743
2	125	1220	3.56	752
3	150	1200	4.04	821
4	175	1260	4.52	896
5	200	1190	5.41	982



6.16 Effective-stress vs. cutting speed



6.18 Temperature vs. cutting speed



6.17 Effective-strain vs. cutting speed

Fig.6.18 shows that when the cutting speed increases, the generated temperature on chip also increases. Where the maximum temperature of the chip formed are increasing with increasing in cutting speed. The increase of cutting speed from 100 m/min to 200 m/min resulted in increases of chip temperature from 743°C to 1120°C. This is due to the increase of required energy at high cutting speed. More heat will be generated as cutting speed increases, consequently the maximum temperature on the tool and workpiece surface increase at higher cutting speed.

## VII. Conclusion:

3D turning of AISI 1045 steel is simulated using FEM code of DEFORM software. The effective stress, effective strain and temperature variation are analyzed and the conclusions are as follows. The simulation of the chip formation, development of temperature distributions as well as predictions of the stress distributions and strain distribution in the chip on the machined surface are successfully achieved. The zone of elevated stress corresponding to intense deformation is located around the primary deformation Zone. Increases in cutting speed while turning AISI 1045 using PCBN tool will decrease the effective- stress to 1190 Mpa. Cutting temperature on the chips formed is increases with the cutting speed from 743 °C to 1120 °C.

## References

- [1] DEFORM-3D Version 10 user Manual.
- [2] *Using Virtual Manufacturing Simulation In 3D Cutting Forces prediction* by Gabriela Patrascu, of the ORADEA UNIVERSITY Fascicle of Management and Technological Engineering, Volume VI (XVI), 2007
- [3] K.C. Jain and A.K Chitale, *A Text book of Production Engineering, Eastern Economy Edition*
- [4] Dr. P.C. Sharma, *A Text book of Manufacturing Technology*, S.Chand Publications.
- [5] J.S. Strenkowski, J.T Carroll, *A Finite Element Model of Orthogonal Metal Cutting*, ASME Trans. J. Engineering for Industry, (1985) Vol. 107. 349-354
- [6] K.Komopoulos, S.A Erpenbeck, *Finite Element Modeling of Orthogonal Cutting*, ASME J. Eng. Ind. 113 (1991) 253-267
- [7] Y. Karpat, T. Özel\* *Process simulations for 3D turning using uniform and variable micro geometry PCBN tools*, Int. J. Machining and Mach inability of Materials, Vol. 3, No. 3, 2008
- [8] Ceretti, E., Lazzaroni, C., Menegardo, L. and Altan, T. (2000) 'Turning simulations using a three-dimensional FEM code', Journal of Materials Processing Technology, Vol. 98, pp.99–103.
- [9] Guo, Y. and Dornfeld, D.A. (1998) 'Finite element analysis of drilling burr minimization with a backup material', Transactions of NAMRI/SME, Vol. 26, pp.207–212.
- [10] Guo, Y. and Liu, C.R. (2002) '3D FEA modeling of hard turning', ASME Journal of Manufacturing Science and Engineering, Vol. 124, pp.189–199.
- [11] Karpat, Y. and Özel, T. (2007) '3-D FEA of hard turning: investigation of PCBN cutting tool
- [12] Kalhori. V. 2001, *Modeling and Simulation of Mechanical Cutting*, Doctoral Thesis, Institutionen for Maskinteknik
- [13] Noordin, M.Y., Venkatesh, V.C., Sharif, S., Elting, S., Abdullah, A., 2003. *Application of response surface methodology in describing the performance of coated carbide tools when turning AISI 1045 steel* Journal of Material Processing Technology, Vol. 145, No. 1, pp. 46- 58, 2004.